Soft-mode splitting in the low-temperature phase of $K_{1-x}Li_xTaO_3$: a comparative Raman and hyper-Raman study

2001 J. Phys.: Condens. Matter 13 4313

(http://iopscience.iop.org/0953-8984/13/19/311)

INSTITUTE OF PHYSICS PUBLISHING JOURNAL OF PHYSICS: CONDENSED MATTER

J. Phys.: Condens. Matter **13** (2001) 4313–4322 www.iop.org/Journals/cm PII: S0953-8984(01)20977-1

Soft-mode splitting in the low-temperature phase of $K_{1-x}Li_xTaO_3$: a comparative Raman and hyper-Raman study

H Vogt

Max-Planck-Institut für Festkörperforschung, Heisenbergstrasse 1, D-70569 Stuttgart, Germany

E-mail: vogt@cardix.mpi-stuttgart.mpg.de

Received 16 January 2001

Abstract

Hyper-Raman measurements on single crystals of $K_{1-x}Li_xTaO_3$ with $x = 0.016$ and 0.043 are supplemented by Raman spectra obtained in the same way as the hyper-Raman data after doubling the laser frequency by an external harmonic generator. The hyper-Raman line of the zone-centre soft mode is compared with the impurity-induced first-order Raman feature resulting from the Raman activation of the whole soft-mode phonon branch. Attention is focused on the frequency splitting as an indicator of tetragonal order around the off-centre Li impurities in the low-temperature phase, to which the samples are cooled down either in the presence or absence of an electric field. Raman scattering is found to probe the tetragonal symmetry of point group C_{4v} at an earlier stage of evolution, i.e. at smaller values of the dipolar correlation length than hyper-Raman scattering. This result is traced back to the different phonon-wavevector selection rules underlying both scattering processes.

1. Introduction

In the last decade, the concept of nanometre-scale polar regions, also called ferroelectric nano-domains or nanometre-sized superparaelectric clusters, has stimulated many investigations of relaxor ferroelectrics [1]. It has also been found useful for describing the evolution of polar order from randomly distributed dipoles in quantum paraelectrics [2–5]. Consistently, Toulouse *et al* [6–8] have combined both fields and have classified $K_{1-x}Li_xTaO_3$ (KLT) and $KTa_{1-x}Nb_xO_3$ (KTN) as relaxors since these solid solutions exhibit similar characteristics in their dielectric, piezoelectric, and elastic response to lead-based prototype relaxors like $PbMg_{1/3}Nb_{2/3}O_3$ (PMN).

It has been noted that the presence of nano-domains excludes a soft-mode triggered phase transition in relaxor ferroelectrics [9]. Indeed, inelastic neutron scattering data obtained for PMN in its high-temperature phase [10] could be interpreted by the assumption that nano-domains in this material stop the softening of a strongly damped quasi-optic excitation and give rise to a central peak. Moreover, evidence was found that nano-domains in PMN act

0953-8984/01/194313+10$30.00

as scattering centres for nanometre-wavelength acoustic phonons and increase their damping. Very recently, a spectacular anomaly has been discovered in the low-frequency transverse optic (TO) phonon branch of the relaxor ferroelectric $Pb(Zn_{1/3}Nb_{2/3})_{0.92}Ti_{0.08}O_3$ [11]. Near the centre of the Brillouin zone, inelastic neutron scattering has revealed a ridge of enhanced phonon scattering cross section which appears as a sudden drop of the TO phonon branch down to the acoustic one. It has been suggested that such a behaviour is the result of polar nano-domains the size of which ($\approx$3 nm) can be estimated from the wavevector at which the drop occurs.

In this paper, we study the influence of nano-domains in KLT on the soft-mode branch in the wavevector range accessible to first-order Raman and hyper-Raman scattering. The former process is strictly forbidden for the cubic perovskite structure of the $KTaO_3$ host lattice and hence probes the soft-mode branch as far as it is Raman activated by the Li-induced disturbance of translational and point-group symmetry. The latter process is already symmetry allowed in undoped $KTaO_3$ [12] and continues to probe the $q = 0$ excitation in KLT.

There is no doubt that the off-centre displacement of the Li^+ impurity acts as the nucleus for the formation of polar order in KLT. Due to its small ionic radius Li^+ does not match the centrosymmetric lattice site of the K^+ ion it substitutes for, but is shifted by roughly a quarter of the lattice constant along one of the six equivalent $\langle 100 \rangle$ directions [13, 14]. Taking into account the associated lattice relaxation, we may refer to Li^+ as a dipole at the core of a polarization cluster of locally tetragonal symmetry [2, 5, 15].

At elevated temperatures and Li concentrations x below about 0.07 [16] the global symmetry of KLT remains cubic because the Li-induced polarization clusters fluctuate independently between their six equivalent orientations. With decreasing temperature, however, the instability of the $KTaO_3$ host lattice with respect to its soft mode leads to an expansion of the polarization clusters [5, 17] and to a modification of the dipole–dipole interaction between them [2, 18]. Finally, both effects end up in a freezing of the Li subsystem into a new low-temperature phase. Depending on the Li concentration, this phase exhibits features of a dipolar glass or a mesoscopic ferroelectric [19]. Accordingly, the phase transition temperature is referred to by various notations, in particular T_g, T_f, and T_c where the subscripts stand for glass, freezing, condensation, characteristic, and Curie, respectively.

The mutual alignment of the polarization clusters due to their soft-mode mediated interaction has to be described by two correlation lengths or order parameters: a *quadrupolar* one ξ_q specifying the range of either parallel or antiparallel orientation (quadrupolar domain) and a *dipolar* one ξ_d measuring the size of the region in which the dipoles point in exactly the same direction (dipolar domain). After cooling below the phase transition temperature in the absence of an externally applied electric field (zero-field cooling (ZFC)), the quadrupolar domains reach macroscopic dimensions and are characterized by a non-vanishing root-mean-square (RMS) polarization, i.e. by $\sqrt{\langle P^2 \rangle} \neq 0$ in spite of $\langle P \rangle = 0$, as evidenced by the onset of birefringence [3, 19, 20]. On the other hand, the dipolar domains remain within the nanometre length scale [3, 5, 21], and only after cooling in the presence of an externally applied electric field (field cooling (FC)), a polarization $\langle P \rangle \neq 0$ due to macroscopic dipolar domains can be detected [13].

Since both kinds of domain reduce the symmetry from cubic to tetragonal, they are expected to split the soft mode of the host crystal into an A and E component denoting vibrations parallel and perpendicular to the tetragonal axis, respectively. In fact, early measurements [22] of Li-induced first-order Raman features have already revealed such a splitting under ZFC conditions in the low-temperature phase of KLT with $x = 0.054$. In addition, a line width broadening observed for $x = 0.022$ has been interpreted as an unresolved splitting. These results appear to have been clearly confirmed by inelastic neutron scattering data. Toulouse

and Hennion [23] have found a split TA phonon branch for $x = 0.035$ after both ZFC and FC. The splitting has been observable down to a reduced wavevector of 0.05 corresponding to a phonon wavelength of about 8 nm. For $x = 0.05$ and ZFC, Klein *et al* [24] have measured a shoulder in the energy distribution of the neutron groups probing the soft-mode branch at the smallest adjustable momentum transfer and interpreted it as splitting of the soft mode even at the very centre of the Brillouin zone.

Surprisingly, no soft-mode splitting after ZFC has been detected in the hyper-Raman spectrum of KLT for Li concentrations up to $x = 0.087$ [5, 25]. The temperature dependence of the soft-mode frequency plotted for various Li concentrations does not show any anomaly indicating a change of symmetry and behaves as if a phase transition does not occur at all. It has been suggested [5, 25], that the ratio λ_{ph}/ξ of phonon wavelength λ_{ph} selected by the scattering technique to correlation length ξ (either quadrupolar or dipolar) may be the criterion for observing a soft-mode splitting. In the case of hyper-Raman scattering, λ_{ph} has been about 120 nm [5] or 170 nm [25], and the absence of a soft-mode splitting may be explained by the assumption that the macroscopic quadrupolar domains do not give rise to a resolvable splitting whereas the tetragonal symmetry of the dipolar domains cannot be probed because their size remains at least one order of magnitude smaller than λ_{ph}. As will be elaborated later, Li-induced first-order Raman scattering selects values of λ_{ph} which are determined just by the size of the region in which the symmetry of the host crystal is disturbed and Raman scattering is no longer forbidden. Hence the ratio λ_{ph}/ξ_d is around 1 for Raman scattering and the detection of a phonon splitting is favoured much more than in the hyper-Raman case. With regard to neutron scattering, it has been pointed out [25] that measurements with a limited wavevector resolution may reveal a soft-mode splitting at $q = 0$ although it is absent right at $q = 0$ or at the reduced wavevector of 0.0024 selected by the hyper-Raman scattering geometry.

In this paper, we intend to improve the experimental basis of the argument outlined above. We present a comparison of Raman and hyper-Raman measurements carried out on the same KLT samples under almost identical conditions after both ZFC and FC. After describing the details of our experimental procedure and the difficulties in preparing a well defined low-temperature phase in section 2, we display our experimental data in section 3 where we also specify the reasons why Raman scattering reveals a soft-mode splitting at smaller values of the dipolar correlation length than hyper-Raman scattering. A preliminary report on some of our results has recently been published in a conference contribution [26].

2. Experimental details

Measurements are carried out on two single crystals of KLT with Li concentrations $x = 0.016$ and 0.043. The phase transition temperatures are around 35 and 65 K, respectively, as deduced from birefringence [22] and hyper-Rayleigh scattering [5]. The samples are parallelepipeds with edges along the $\langle 100 \rangle$ directions, with edge lengths varying between 3 and 6 mm. An electric dc field can be applied to the largest pair of opposite faces via silver-paste electrodes. The crystals are mounted on a Teflon insulated sample holder in a continuous-flow cryostat and cooled by helium exchange gas. To prevent glow discharge within the exchange gas, the electrodes are coated with a varnish (General Electric 7031). This varnish is also used for improving the thermal contact between sample and holder.

Details of our hyper-Raman spectrometer have been described elsewhere [17]. The conventional single-channel technique combining a scanning double-monochromator, a Burle/RCA C31034 photomultiplier tube and gated photon-counting equipment is applied. The source of the exciting radiation is an acousto-optically Q-switched diode-laser-pumped

Nd-YAG laser (Coherent model DPY 501 QII) providing laser pulses of 1.064 μm wavelength, 30 ns width, and 3.2 kHz repetition rate. The average laser power at the site of the sample has to be kept below about 200 mW in order to avoid self-focusing effects in the low-temperature phase which are noticed by deviations from the quadratic relation between hyper-Raman signal and average laser power and finally result in optical damage.

We easily switch from hyper-Raman to Raman scattering by inserting an external KD*P (potassium dideuterium phosphate) frequency doubler into the path of the laser beam and exchanging appropriate Schott filters. No readjustment of sample and electronics is found to be necessary at a spectral slit width of about 2–3 cm^{-1}. The Raman spectra are registered with an average power of about 1 mW at the site of the sample.

To some unknown extent, the reproducibility of all measurements in the low-temperature phase of KLT seems to be limited by metastability and non-ergodicity which have recently become the subject of extensive research [27, 28]. In order to exclude non-ergodicity and ageing effects from our results as much as possible, we always keep to the same thermal treatment: cooling down from room temperature at a rate of about 1 K min^{-1}, waiting for about 1 h at the final temperature before starting the measurement, and slowly warming up to room temperature afterwards. For measurements under FC conditions, we apply the electric field at about 120 K during the cooling process, while we switch it off and short-circuit the electrodes when the sample returns to room temperature.

Another severe problem may arise from the unexpectedly high photoconductivity of KLT in its low-temperature phase. The photoconductivity results from Li-induced shallow hole traps preventing the recombination of electron–hole pairs which are probably created at uncontrolled Fe^{2+}/Fe^{3+} centres in a multi-step excitation process [29, 30]. During laser illumination, the photoexcited carriers may build up a space charge influencing the evolution of polar order. According to Banfi *et al* [31] space charge effects do not play any significant role at the wavelength of the Nd-YAG laser because the photon energy is too small to create a sufficient number of electron–hole pairs. At the wavelength of the second harmonic, however, an external poling field screens itself by drifting photoexcited carriers from the interior to the edge of the illuminated region [31]. For this reason, we have to adopt the following procedure for *Raman* measurements under FC conditions: cooling down in the dark and switching off the electric field *before* starting the Raman measurement. Of course, the Raman results thus obtained seem to be reliable only at sufficiently low temperatures where the alignment of the Li-dipole system is frozen in to such an extent that it does not change when the poling field is removed.

3. Results and discussion

In figures 1 and 2 we compare Raman and hyper-Raman spectra of $K_{0.984}Li_{0.016}TaO_3$ at 15 K after both ZFC and FC. The 90° scattering geometries are described in Porto's notation, the cubic axes of the high-temperature phase being denoted by *X*, *Y*, and *Z*.

After ZFC the hyper-Raman spectrum displays a single well defined soft-mode hyper-Raman line in contrast to the Li-induced Raman feature which appears as a broad asymmetric hump superimposed on the second-order Raman spectrum. A Raman band of this type can be described in terms of a 'degenerate' second-order Raman effect in which the static or quasistatic lattice distortions due to polarization clusters or ferroelectric nano-domains combine as zero-frequency excitations with the phonons of the soft-mode branch to give combination tones just

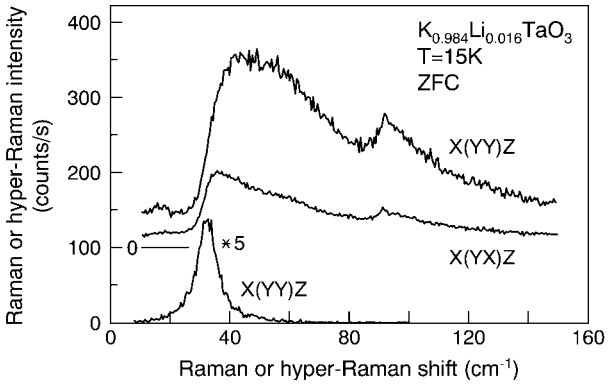

Figure 1. Raman (upper curves) and hyper-Raman (lower curve) spectra of $K_{0.984}Li_{0.016}TaO_3$ at a temperature of 15 K after cooling in the absence of any externally applied electric field (zero-field cooling, ZFC). The scattering geometries are explained in the text. The scaling factor indicates an amplification of the hyper-Raman line by a factor of five.

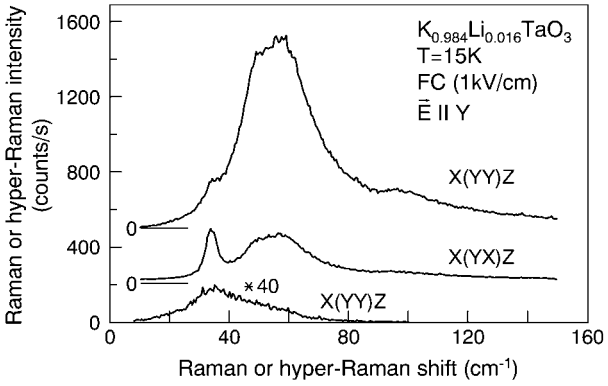

Figure 2. Raman (upper curves) and hyper-Raman (lower curve) spectra of $K_{0.984}Li_{0.016}TaO_3$ at a temperature of 15 K after cooling in the presence of an electric field strength of 1 kV cm^{-1} externally applied along the [010] or *Y* direction (FC). The scattering geometries are explained in the text. The scaling factor indicates an amplification of the hyper-Raman line by a factor of 40.

at the phonon frequencies [32–34]. The Raman intensity $I_R(\omega)$ is then given by

$$I_R(\omega) \propto \sum_{\boldsymbol{q}} \eta_0(\boldsymbol{q} - \boldsymbol{K})\ \eta_0(-\boldsymbol{q} + \boldsymbol{K})\ \langle \eta'(\boldsymbol{q}, \omega)\ \eta'(-\boldsymbol{q}, -\omega)\rangle \tag{1}$$

where we follow the notation of Levanyuk *et al* [32] and divide the relevant lattice distortions into a fluctuating part η' resulting from the phonons of the soft-mode branch and a Li-induced quasistatic part η_0 which Raman activates the phonons. For the sake of simplicity, we confine the thermal average to the phonon terms and assume η_0 to be constant in time because the flipping motions of the Li dipoles are very slow compared to the vibrations of the soft-mode branch. The sum is over all wavevectors $\boldsymbol{q}$ belonging to phonons of frequency $\omega(\boldsymbol{q})$. The difference between the wavevectors of the incident and scattered light is taken into account by $\boldsymbol{K} \approx 0$. Introducing the one-phonon density of states $D(\omega)$ of the soft-mode branch, we

obtain

$$I_R(\omega) \propto \frac{n(\omega, T) + 1}{\omega} D(\omega) \sum_{\boldsymbol{q}_\omega} \eta_0(\boldsymbol{q}_\omega)\, \eta_0(-\boldsymbol{q}_\omega) \tag{2}$$

where $n(\omega, T)$ is the Bose–Einstein population factor and $\boldsymbol{K} \approx 0$ has been neglected. A subscript ω is affixed to $\boldsymbol{q}$ to indicate that the summation over $\boldsymbol{q}$ has to be restricted to phonons of frequency ω.

According to equation (2) the leading edge of the Raman band in figure 1 reflects the increasing density of states $D(\omega)$, while the length of the trailing edge is determined by the dispersion $\omega(\boldsymbol{q})$ and the spectrum of $\boldsymbol{q}$ values characterizing the shape and size of the polarized regions. Assuming a correlation length ξ_d of approximately 5 nm as evaluated previously [3, 5], we expect the soft-mode branch to be Raman activated for reduced wavevectors below about $a/\xi_d \approx 0.08$ (a = lattice constant). From the dispersion curve obtained by inelastic neutron scattering for a Li concentration of $x = 0.01$ [24], we estimate that the Li-induced Raman band should extend at least up to 75 cm^{-1} in reasonable agreement with figure 1 where the overtone of zone-boundary TA phonons around 90 cm^{-1} interferes with the high-frequency tail of the Raman band of interest.

After FC the soft-mode hyper-Raman line becomes broadened whereas the Li-induced Raman feature is not only intensified by a factor of 3–4, but also reveals a splitting of the soft-mode branch. The relative intensities of the two components can already be related to the Raman symmetry selection rules of point group C_{4v} with the tetragonal axis parallel to the electric field. In the presence of perfect C_{4v} symmetry, the higher-frequency A_1 component should be restricted to the scattering geometry $X(YY)Z$, whereas the lower-frequency E component should only appear in the $X(YX)Z$ spectrum (see for example reference [35]). Although these requirements are far from being strictly fulfilled, they seem to be approached in figure 2.

In contrast to the Raman results, the hyper-Raman data do not give any evidence of C_{4v} symmetry. Since the scattering geometry $X(YY)Z$ selects a phonon with an eigenvector parallel to the Y axis and a wavevector in the $[10\bar{1}]$ direction, we expect the soft-mode hyper-Raman line at the position of the A_1 component around 55 cm^{-1}, if a perfect C_{4v} symmetry is induced by the electric field, or a splitting into two components, if the crystal is divided into macroscopic dipolar domains aligned along the X, Y, and Z axes, perhaps with preference of the second one. Neither expectation is confirmed. We have to conclude that ξ_d is still far below 170 nm, i.e. the wavelength of the phonon probed by hyper-Raman scattering, but well above 5 nm as indicated by the splitting of the Raman band.

In figures 3–5, we plot the Raman and hyper-Raman spectra of $K_{0.957}Li_{0.043}TaO_3$ at four different temperatures above and below the phase transition around 65 K. All data refer to ZFC.

In agreement with reference [22], we observe a splitting of the Li-induced Raman band already in the absence of any external electric field. On the other hand, we confirm our previous result [5, 25] that only a single soft-mode line appears in the hyper-Raman spectrum. There is almost no hyper-Raman signal at about 80 cm^{-1} where the higher-frequency component of the Raman band is observed. According to reference [3], the dipolar correlation length ξ_d has a value between 12 nm ($x = 0.034$) and 23 nm ($x = 0.06$). Combining this order of magnitude ξ_d with the experimental findings of figures 3–5, we have to infer that at temperatures below 15 K the soft-mode branch starts at the Γ point with a frequency of about 40 cm^{-1}, but then develops a second component at almost twice the frequency somewhere in the reduced-wavevector range between 0.002 and 0.03. In view of recent neutron scattering results mentioned in the introductory section [11], we should not only take into consideration

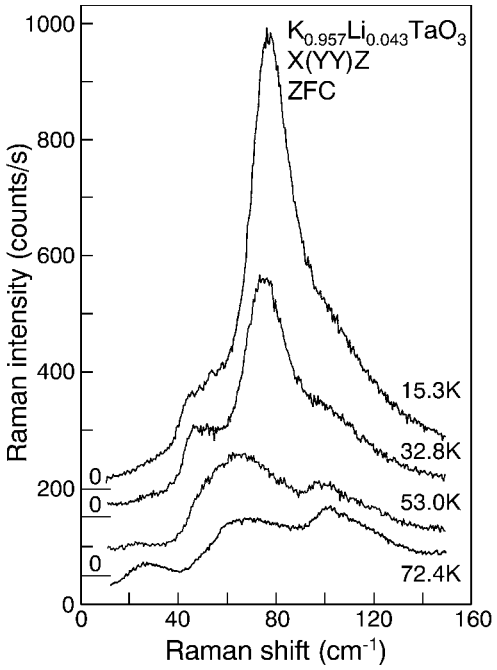

Figure 3. Raman spectra of $K_{0.957}Li_{0.043}TaO_3$ at four different temperatures after cooling without external electric field (ZFC).

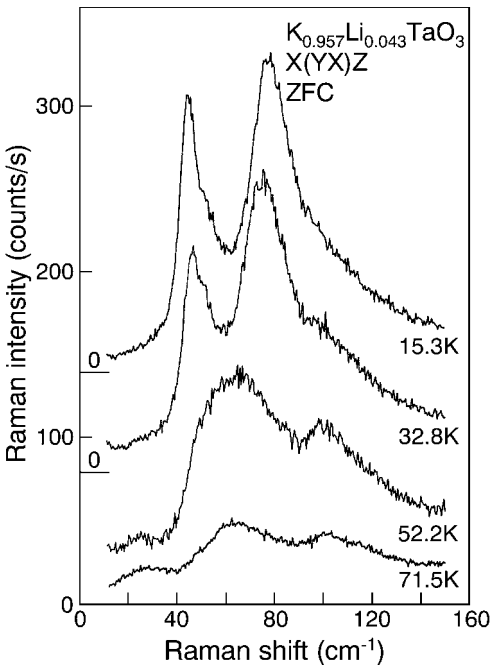

Figure 4. Raman spectrum of $K_{0.957}Li_{0.043}TaO_3$ after ZFC as a function of temperature. Compared to figure 3, a different scattering geometry is used.

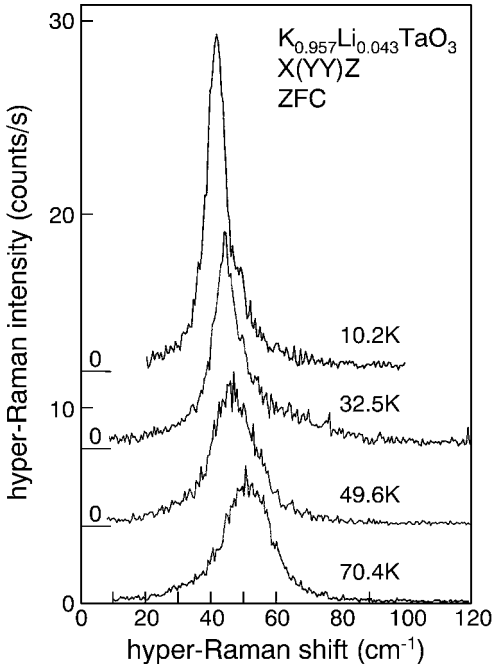

Figure 5. Hyper-Raman spectra of $K_{0.957}Li_{0.043}TaO_3$ obtained after ZFC from room temperature to four different temperatures above and below the phase transition.

a continuous phonon dispersion curve branching at a certain wavevector. It may also be possible to explain the lack of one component in the hyper-Raman spectra by overdamping in a wavevector region determined by the dipolar correlation length ξ_d.

As shown by figures 2 and 5, the soft-mode hyper-Raman line is observed at the spectral position of the lower-frequency E component of the Raman band. It does not represent an average over the E and A_1 components of the Raman band with some intermediate frequency. Thus we are led to the conclusion that it is the A_1 phonon, i.e. the phonon with an eigenvector parallel to the polarization of the dipolar nano-domains, which is sensitive to the size of the nano-domains characterized by ξ_d. For $\lambda_{ph}/\xi_d \gg 1$, the A_1 phonon of wavelength λ_{ph} either coincides with the E phonon or cannot propagate at all due to overdamping.

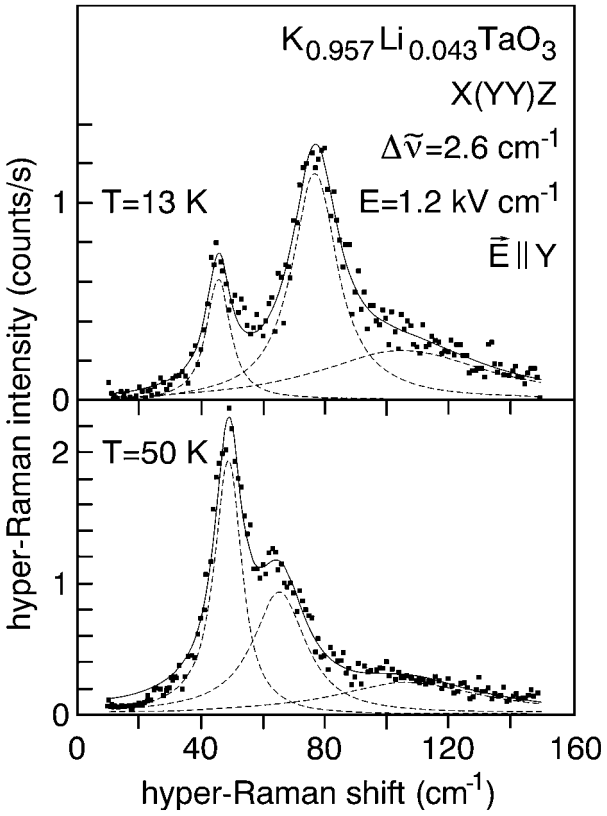

Figure 6. Hyper-Raman spectra of $K_{0.957}Li_{0.043}TaO_3$ at 13 and 50 K after cooling the sample through the phase transition in the presence of an external field of 1.2 kV (FC). The solid lines are fits of a three-oscillator spectral function to the experimental points. The broken lines indicate the individual contributions of the three oscillators.

The opposite case is demonstrated in figure 6 where we show that a soft-mode splitting is indeed detected by hyper-Raman spectroscopy as soon as ξ_d reaches or exceeds the order of magnitude of the phonon wavelength of about 170 nm selected by the scattering geometry. For a Li concentration of $x = 0.043$, the A_1–E doublet can clearly be resolved after FC even at 50 K. Attempting to describe our experimental data by simple spectral functions, we find a two-oscillator fit to be insufficient because it does not take into account the high-frequency shoulder of the A_1 component. This shoulder most probably reflects the frequency-dependent self-energy of the soft mode and seems to be related to the maximimum of the two-phonon

density of states giving rise to the band at the same spectral position in the Raman spectra of figures 1–4. For simulating the shoulder, we supplement the two oscillators of the doublet by a third oscillator of temperature-independent frequency and damping constant, thus obtaining fits of a *three*-oscillator spectral function to the experimental points as indicated by the solid lines in figure 6. The broken lines represent the individual contributions of the three oscillators.

If the external electric field completely aligns the Li-dipole system, only the A_1 component is predicted for the scattering geometry $X(YY)Z$. As shown by figure 6, this ideal case cannot be realized by an electric field strength of 1.2 kV cm^{-1}. However, the change of the relative intensities of the two components of the doublet with decreasing temperature, clearly indicates that preference is given to domains polarized in the direction of the poling field.

4. Summary

The signatures of the soft mode in the Raman and hyper-Raman spectra of $K_{1-x}Li_xTaO_3$ with $x = 0.016$ and 0.043 are compared with each other. An attempt is made to specify the conditions under which a soft-mode splitting becomes observable in the low-temperature phase to which the samples are cooled down with and without a poling electric field. Evidence is found that the A_1 component of the soft mode with an eigenvector parallel to the polarization of the dipolar nano-domains is sensitive to the size of the nano-domains characterized by the dipolar correlation length ξ_d. A distinct A_1 phonon clearly separated from its E counterpart is only observable if its wavelength λ_{ph} is smaller than ξ_d or has the same order of magnitude. In the opposite case, i.e. for $\lambda_{ph}/\xi_d \gg 1$, no frequency splitting can be detected because the A_1 phonon either coincides with the E phonon or cannot propagate at all due to overdamping. Since Li-induced first-order Raman scattering probes phonons of smaller wavelength than hyper-Raman scattering, the Raman spectra display a soft-mode doublet always at an earlier stage in the evolution of polar order, i.e. at smaller values of ξ_d, than the hyper-Raman spectra.

Acknowledgments

The author wishes to thank S Kapphan (Universität Osnabrück, Germany) for kindly providing the samples and J Kuhl for a critical reading of the manuscript.

References

[1] Cross L E 1994 *Ferroelectrics* **151** 305–20
[2] Vugmeister B E and Glinchuk M D 1990 *Rev. Mod. Phys.* **62** 993–1026
[3] Azzini G A, Banfi G P, Giulotto E and Höchli U T 1991 *Phys. Rev.* B **43** 7473–80
[4] DiAntonio P D, Vugmeister B E, Toulouse J and Boatner L A 1993 *Phys. Rev.* B **47** 5629–37
[5] Vogt H 1995 *J. Phys.: Condens. Matter* **7** 5913–29
Vogt H 1996 *Ferroelectrics* **184** 31–9
[6] Toulouse J, Vugmeister B E and Pattnaik R 1994 *Phys. Rev. Lett.* **73** 3467–70
[7] Pattnaik R and Toulouse J 1997 *Phys. Rev. Lett.* **79** 4677–80
[8] Toulouse J and Pattnaik R 1998 *J. Korean Phys. Soc.* **32** S942–6
[9] Tsurumi T, Soejima K, Kamiya T and Daimon M 1994 *Japan. J. Appl. Phys. Part I* **33** 1959–64
[10] Naberezhnov A, Vakhrushev S, Dorner B, Strauch D and Moudden H 1999 *Eur. Phys. J.* B **11** 13–20
[11] Gehring P M, Park S-E and Shirane G 2000 *Phys. Rev. Lett.* **84** 5216–9
[12] Vogt H 1988 *Phys. Rev.* B **38** 5699–708
[13] van der Klink J J, Rytz D, Borsa F and Höchli U T 1983 *Phys. Rev.* B **27** 89–101
[14] Eglitis R I, Postnikov A V and Borstel G 1998 *Phys. Status Solidi* b **209** 187–93

[15] van der Klink J J and Khanna S N 1984 *Phys. Rev.* B **29** 2415–22
[16] Geifman I N, Kozlova I V, Konovalov K I, Son'ko T V and Furmanova N G 1990 *Sov. Phys. Crystallogr.* **35** 427–31
[17] Vogt H 1998 *Phys. Rev.* B **58** 9916–25
[18] Vugmeister B E 1991 *Ferroelectrics* **120** 133–40
[19] Kleemann W, Kütz S and Rytz D 1987 *Europhys. Lett.* **4** 239–45
[20] Courtens E 1981 *J. Phys. C: Solid State Phys.* **14** L37–42
[21] Banfi G P, Calvi P and Giulotto E 1995 *Phys. Rev.* B **51** 6231–36
[22] Prater R L, Chase L L and Boatner L A 1981 *Phys. Rev.* B **23** 5904–15
[23] Toulouse J and Hennion B 1994 *Phys. Rev.* B **49** 1503–6
[24] Klein R S, Kugel G E and Hennion B 1996 *J. Phys.: Condens. Matter* **8** 1109–21
[25] Vogt H 1997 *Ferroelectrics* **202** 157–65
[26] Vogt H 2000 *Ferroelectrics* **239** 165–172
[27] Alberici-Kious F, Bouchaud J P, Cugliandolo L F, Doussineau P and Levelut A 1998 *Phys. Rev. Lett.* **81** 4987–90
[28] Doussineau P, de Lacerda-Arôso T and Levelut A 2000 *J. Phys.: Condens. Matter* **12** 1461–71
[29] Klein R S, Kugel G E, Glinchuk M D, Kuzian R O and Kondakova I V 1994 *Phys. Rev.* B **50** 9721–8
[30] Sangalli P, Giulotto E, Rollandi L, Calvi P, Camagni P and Samoggia G 1998 *Phys. Rev.* B **57** 6231–4
[31] Banfi G P, Calvi P, Camagni P, Giulotto E, Rollandi L, Samoggia G and Sangalli P 1997 *J. Phys.: Condens. Matter* **9** 507–14
[32] Levanyuk A P, Sigov A S and Sobyanin A A 1983 *Light Scattering near Phase Transitions* ed H Z Cummins and A P Levanyuk (Amsterdam: North-Holland) p 145
[33] Uwe H, Lyons K B, Carter H L and Fleury P A 1986 *Phys. Rev.* B **33** 6436–40
[34] Calvi P, Camagni P, Giulotto E and Rollandi L 1996 *Phys. Rev.* B **53** 5240–6
[35] Manlief S K and Fan H Y 1972 *Phys. Rev.* B **5** 4046–60